

Whole-body Averaged SAR Assessment Using a Personal, Distributed Exposimeter

Arno Thielens¹, Peter Vanveerdeghem², Sam Agneessens², Patrick Vantorre², Günter Vermeeren¹, Hendrik Rogier², Luc Martens¹, and Wout Joseph¹

Department of Information Technology, Ghent University / iMinds, Ghent, Belgium

*Corresponding author e-mail: Arno.Thielens@intec.UGent.be

SHORT ABSTRACT

The whole-body averaged specific absorption rate (SAR_{wb}) can be estimated using a personal, distributed exposimeter (PDE) when combining a calibration using the PDE and numerical simulations. A PDE for the Global System for Mobile Communications (GSM) 900 downlink band is constructed using 4 textile antennas and 4 radio frequency (RF) receiver nodes. Calibration measurements at 942.5 MHz, using a human subject, are performed in an anechoic chamber. The PDE has a 50% prediction interval caused by the human body on SAR_{wb} of 3.3 dB. Measurements using the PDE are carried out in Ghent (Belgium), during which a median $S_{inc}=47 \mu W/m^2$ and $SAR_{wb}=0.25 \mu W/kg$ are measured

INTRODUCTION

The absorption of Radio Frequency (RF) electromagnetic fields (EMFs) can be studied using the whole-body averaged specific absorption rate (SAR_{wb}), for which basic restrictions (BRs) are issued by the International Commission on Non-Ionizing Radiation Protection (ICNIRP) [1]. The SAR_{wb} is usually studied using numerical simulations [2], but cannot be measured inside living humans. Therefore, reference levels (RLs) on the incident power densities (S_{inc}), which can be measured, have been derived from the BRs [1]. This S_{inc} is frequently measured using personal exposimeters (PEMs) [3-6]. PEMs are typically worn on-body and allow for an instantaneous assessment of personal exposure to RF EMFs. However, they are faced with relatively large measurement uncertainties caused by the presence of the human body [3-5]. A personal, distributed exposimeter (PDE) can be used to reduce this uncertainty [5]. In [5], a PDE has been demonstrated using measurements in an anechoic chamber, but has not been used outside the lab. A method to determine statistics for the SAR_{wb} from PEM measurements has been proposed in [6], but is faced with the same large measurement uncertainties of PEMs. In this study, a personal whole-body averaged SAR meter is proposed, which estimates SAR_{wb} with a lower measurement uncertainty using a PDE. This device enables epidemiologists to not only relate health effects to incident field levels, but to absorption levels as well.

MATERIALS AND METHODS

A PDE is constructed, calibrated, and used for actual measurements of the S_{inc} and SAR_{wb} in the Global System for Mobile Communications (GSM) 900 downlink (DL) band: 915-960 MHz.

The PDE consists of 4 RF acquisition nodes. Every node is a combination of a textile antenna connected to an RF power detection unit tuned to the GSM 900 DL band. The used linearly polarized textile antenna is a quarter wavelength planar inverted F antenna (PIFA). The RF power detection unit records the received power ($P_{r,i}$) on textile antenna i ($i=1..4$) and

provides a geometric averaged received power with a resolution of 1 dB, a sensitivity of -72 dBm, and a sample interval of 1 Hz. The nodes are powered individually and are synchronized at start-up, avoiding interconnections and thus allowing real-life measurements. The RF nodes are lightweight, do not interfere with body movement, and have a surface of 10 x 12 cm².

The PDE, worn by a 26 year old male subject with a body mass index (BMI) of 22.6 kg/m², is calibrated in an anechoic chamber. A calibration procedure is proposed to simultaneously determine where the RF nodes should be placed on the subject's body and what the effective on-body antenna aperture (AA) of this configuration is. First, the (linearly polarized) RF nodes are placed both horizontally (H), parallel to the subject's transverse plane and vertically (V), orthogonal to the subject's transverse plane, on a 2x2x3 grid on the front and back of the subject's torso (A to L), shown in Figure 1.

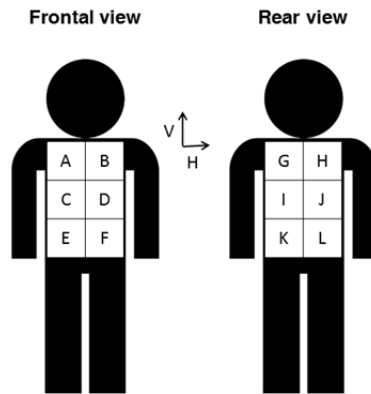


Figure1: Possible locations to deploy the RF acquisition nodes on the subject's body.

The subject is then rotated 360° around his main axis in the far field of a horn antenna (TX) emitting at 942.5 MHz, with an input power of 10 mW. Each rotation is repeated for both H and V polarized TX. This results in 24 measurements of the on-body received power $P_{r,j}^H(\varphi)$ and $P_{r,j}^V(\varphi)$ ($j=1..24$). Second, the free-space S_{inc}^H and S_{inc}^V are measured using a NARDA broadband probe (NBM-550), for both polarizations (H and V) of the TX. Third, $P_{r,j}^H(\varphi)$ and $P_{r,j}^V(\varphi)$ are averaged geometrically over sets of 4 antennas. To this aim, 4 positions are drawn without repetition from the 12 possible on-body positions (C_{12}^4). The possible orientations of the antennas are restricted: 2 antennas have to be H polarized and 2 antennas V polarized, because this configuration is less polarization dependent. This results in 2970 geometric ($P_{geom,l}^H(\varphi)$ and $P_{geom,l}^V(\varphi)$) averaged received powers for $l=1..2970$. These received powers can be used to calculate the geometric averaged AA of the PDE ($AA_{geom,l}$):

$$AA_{geom,l}(\varphi, \psi) = \frac{P_{geom,l}^H(\varphi)}{S_{inc}^H} \cos^2(\psi) + \frac{P_{geom,l}^V(\varphi)}{S_{inc}^V} \sin^2(\psi) \quad (1)$$

with ψ the polarization of an incident electric field. In order to account for a realistic polarization, $AA_{geom,l}(\varphi, \psi)$ is calculated for 10^3 ψ -samples, drawn from a Gaussian distribution for ψ in an "Urban Macro cell" scenario [2]. This scenario is chosen because it corresponds best to the measurements that are carried out with the PDE in Ghent [6]. This procedure is repeated 100 times in order to determine the reproducibility of the distribution of $AA_{geom,l}$. In a fourth step, the combination l with the lowest interquartile distance of its $AA_{geom,l}$ distribution, is chosen. In a final step, the antennas are placed simultaneously on the

subject's body on the selected positions (I) with the selected polarizations. AA_{geom} is measured again in the anechoic chamber and processed using the same calibration procedure. This results, in a cumulative distribution function $Prob(AA_{geom} \leq Z)$. The incident power density can be measured using this distribution:

$$S_{inc} = \frac{P_{geom}}{AA_{geom}} \quad (2)$$

where P_{geom} is the geometric averaged received power during measurements. A distribution $Prob(S_{inc} \leq X | P_{geom} = 1 W)$ can be obtained by inverting $Prob(AA_{geom} \leq Z)$ using Equation (2) with $P_{geom} = 1 W$.

Simultaneously, finite-difference time-domain (FDTD) simulations using the Virtual Family Male (VFM) [7] are executed at 950 MHz. The VFM is a heterogeneous phantom with a BMI= 22.3 kg/m² (± 0.5 kg/m² compared to the subject's BMI). Using the method described in [2], the SAR_{wb} for the VFM can be determined in the same 'Urban Macro cell' environment [2]. To this aim, 5000 multipath exposure samples are generated in this environment, from which a distribution $Prob(SAR_{wb} \leq Y | S_{inc} = 1 W/m^2)$ can be determined [2]. An expression for $Prob(SAR_{wb} \leq Y | P_{geom}^{meas} = 1 W)$ can be found using Bayes Theorem:

$$Prob(SAR_{wb} \leq Y | P_{geom} = 1 W) = \int_0^\infty Prob(SAR_{wb} \leq Y | S_{inc} = X) \times \frac{dProb}{dX}(S_{inc} \leq X | P_{geom} = 1 W) dX \quad (3)$$

In practice, the median values of the distributions $Prob(S_{inc} \leq X | P_{geom} = 1 W)$ and $Prob(SAR_{wb} \leq Y | P_{geom} = 1 W)$ are multiplied by the registered received powers will be used as an estimate of the S_{inc} and SAR_{wb} . The 50 % prediction interval (PI₅₀) of those quantities are the interquartile distances of their distributions determined using Eqs (2) and (3).

Following the calibration measurements, the subject follows a 3.1-km-long outdoor trajectory through Ghent, Belgium, shown in Figure 2 (a). During this walk the powers received on the textile antennas are recorded and averaged over the 4 RF nodes. From these averaged powers S_{inc} and SAR_{wb} values can be determined using the procedure described above. These (median) values are then averaged over 6 minutes and compared to the ICNIRP RLs and BRs [1].

RESULTS

Following the proposed calibration procedure, a geometric averaging of the received power over 4 RF nodes placed horizontally on position B, vertically on D, horizontally on G, and vertically on H (see Figure 1), respectively, is found to lead to the lowest PI₅₀. Table 1 shows the most important performance characteristics of the PDE after the calibration procedure.

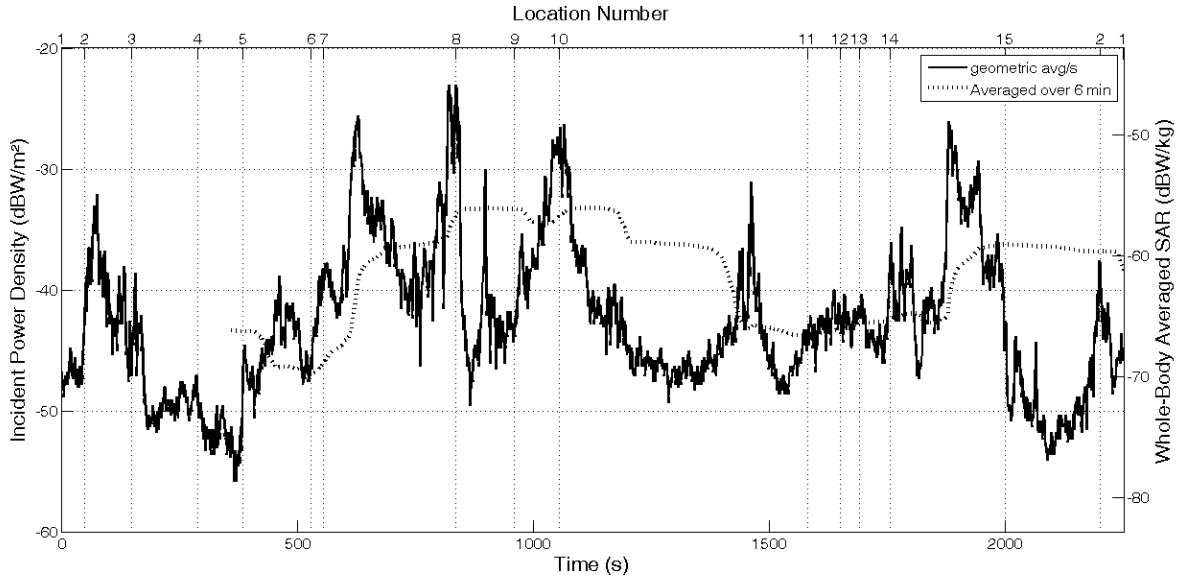
Quantities	Values
Selected positions ^{polarizations}	B ^H , D ^V , G ^H , I ^V
$p_{50}(AA_{geom})$ (cm ²)	6.06 ± 0.05
PI ₅₀ of AA_{geom}/S_{inc} (dB)	3.09 ± 0.02
Detection limit ($\mu W/m^2$)	0.104 ± 0.001
$p_{50}(SAR_{wb} P_{geom} = 1 W)$ (W/kg)	8.7 ± 0.5
PI ₅₀ of SAR_{wb} (dB)	3.3 ± 0.6

Table 1: Performance characteristics of the PDE for the GSM 900 DL band.

As Table 1 shows, the PI_{50} on S_{inc} is 3.1 dB. This value is a measure for the uncertainty caused by the human body and is low compared to the minimal and median values of 7.1 dB and 12 dB, respectively, which are found for the single antennas. Previous studies using PEMs find values for the PI_{50} on measured S_{inc} of 8.0 dB [4] using numerical simulations and 6.5 dB and 16 dB for horizontally and vertically polarized incident fields, respectively, recorded by a PEM worn on the hips [3]. For a previous prototype of the PDE using 3 RF nodes we obtained a PI_{50} of 4.5 dB [5]. All these values are higher than the PI_{50} listed in Table 1. This indicates that the PDE can be used for measurements of S_{inc} with less uncertainty. Moreover, the PI_{50} on the SAR_{wb} distribution of 3.3 dB is also relatively low compared to the minimal and median values of 5 dB and 10 dB, respectively, found for the single antennas. However, it should be noted that there is an additional uncertainty (50 % prediction interval of 1.64 dB) on the numerically obtained SAR_{wb} values.



(a)



(b)

Figure 2: (a) Trajectory followed in Ghent (Belgium) during measurements (source: Google maps 2014). (b) S_{inc} and SAR_{wb} values measured along the trajectory. The location numbers on the upper horizontal axis correspond to those indicated in Fig. 2 (a).

Figure 2 (b) shows the S_{inc} (left vertical axis) and SAR_{wb} (right vertical axis) values that are obtained by geometrically averaging the received powers over the 4 textile antennas with a sample rate of 1 Hz (full line) and averaged over 6 minutes (dashed). All measured data are above the detection limit. A median S_{inc} of $47 \mu\text{W}/\text{m}^2$ and a median $SAR_{wb} = 0.25 \mu\text{W}/\text{kg}$ are measured along the full trajectory using the PDE. The maximally registered values are $S_{inc} = 4.9 \text{ mW}/\text{m}^2$ and $SAR_{wb} = 26 \mu\text{W}/\text{kg}$. All the measured values, and thus also the values averaged over 6 minutes, are lower than the ICNIRP reference levels ($4.8 \text{ W}/\text{m}^2$) and basic restrictions ($0.08 \text{ W}/\text{kg}$) for the general public.

CONCLUSIONS

We propose a calibration method for a personal, distributed exposimeter (PDE) which measures the incident power density (S_{inc}) and **whole-body averaged specific absorption rate (SAR_{wb})**, a SAR_{wb} -meter, in the Global System for Mobile Communications (GSM) 900 downlink (DL) band using 4 radio frequency (RF) power detection nodes combined with 4 textile antennas. The PDE has a relatively low measurement uncertainty caused by the human body: 50 % prediction intervals (PI_{50}) of 3.1 dB on S_{inc} and 3.3 dB on SAR_{wb} are measured for the PDE whereas the best single textile antenna in our measurements has PI_{50} of 7.1 dB on S_{inc} and 5 dB on SAR_{wb} . The PDE is used for real measurements in Ghent (Belgium) where a median S_{inc} of $47 \mu\text{W}/\text{m}^2$ and $SAR_{wb} = 0.25 \mu\text{W}/\text{kg}$ are measured.

ACKNOWLEDGMENT

This research was funded by the FWO under grant agreement No 3G004612.

REFERENCES

- [1] International Commission on Non-Ionizing Radiation Protection. 1998. Guidelines for limiting exposure to time-varying electric, magnetic, and electromagnetic fields (up to 300 GHz). Health Physics 74: 494-522.
- [2] Vermeeren G, Joseph W, Olivier C, Martens L. 2008. Statistical multipath exposure of a human in a realistic

electromagnetic environment, *Health Physics* 94: 345 – 54.

- [3] Bolte J.F.B., Van der Zande G., Kamer J., 2011. Calibration and uncertainties in personal exposure measurements of radiofrequency electromagnetic fields. *Bioelectromagnetics* 32(8): 652-663.
- [4] Neubauer G, Cecil S, Giczi W, Petric B, Preiner P, Fröhlich J, Rösli M. 2010. The association between exposure determined by radiofrequency personal exposimeters and human exposure: a simulation study. *Bioelectromagnetics* 31: 535-545.
- [5] Thielens A, De Clerq H, Agneessens S, Lecoutere J, Verloock L, Declerq F, Vermeeren G, Tanghe E, Rogier H, Puers R, Martens L, Joseph W. 2013. Distributed on Person Exposimeters for Radio Frequency Exposure Assessment in Real Environments. *Bioelectromagnetics* 34 (7):563-567.
- [6] Joseph W, Vermeeren G, Verloock L, Heredia MM, Martens L. 2008. Characterization of Personal RF Electromagnetic Field Exposure and Actual Absorption for the General Public. *Health Physics* 95(3): 317-330.
- [7] Christ A, et al. The Virtual Family - development of surface-based anatomical models of two adults and two children for dosimetric simulations. *Phys Med Biol* 48:N23-N38, 2010.